

RICE UNIVERSITY

On Properties of the Hohmann Transfer

by

Jarret Mathwig

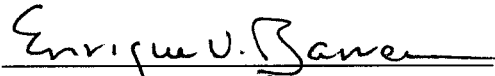
A THESIS SUBMITTED
IN PARTIAL FULFILLMENT OF THE
REQUIREMENTS FOR THE DEGREE

Master of Science

APPROVED, THESIS COMMITTEE:



Angelo Miele, Foyt Professor Emeritus,
Mechanical Engineering and Materials
Science Department



Enrique Barrera, Professor,
Mechanical Engineering and Materials
Science Department



Richard Tapia, Noah Harding Professor
Computational and Applied Mathematics
Department

HOUSTON, TEXAS

APRIL, 2004

UMI Number: 1419106

INFORMATION TO USERS

The quality of this reproduction is dependent upon the quality of the copy submitted. Broken or indistinct print, colored or poor quality illustrations and photographs, print bleed-through, substandard margins, and improper alignment can adversely affect reproduction.

In the unlikely event that the author did not send a complete manuscript and there are missing pages, these will be noted. Also, if unauthorized copyright material had to be removed, a note will indicate the deletion.



UMI Microform 1419106

Copyright 2004 by ProQuest Information and Learning Company.

All rights reserved. This microform edition is protected against unauthorized copying under Title 17, United States Code.

ProQuest Information and Learning Company
300 North Zeeb Road
P.O. Box 1346
Ann Arbor, MI 48106-1346

ABSTRACT

On Properties of the Hohmann Transfer

by

Jarret Mathwig

In this work, we present a complete study of the Hohmann transfer maneuver between two circular coplanar orbits. After revisiting its known properties, we present a number of supplementary properties which are essential to the qualitative understanding of the maneuver. Specifically, along a Hohmann transfer trajectory, there exists a point where the path inclination is maximum: this point occurs at midradius and is such that the spacecraft velocity equals the local circular velocity. This implies that, in a Hohmann transfer, the spacecraft velocity is equal to the local circular velocity three times: before departure, at midradius, and after arrival. In turn, this allows the subdivision of the Hohmann transfer trajectory into a region where the velocity is subcircular and a region where the velocity is supercircular, with the transition from one region to another occurring at midradius.

Also, we present a simple analytical proof of the optimality of the Hohmann transfer and complement it with a numerical study via the sequential gradient-restoration algorithm. Finally, as an application, we present a numerical study of the transfer of a spacecraft from the Earth orbit around the Sun to another planetary orbit around the Sun for both the case of an ascending transfer (orbits of Mars, Jupiter, Saturn, Uranus, Neptune, and Pluto) and the case of a descending transfer (orbits of Mercury and Venus).

Key Words. Flight mechanics, astrodynamics, celestial mechanics, Hohmann transfer maneuver, orbital transfer, ascending transfer, descending transfer.

Acknowledgments

I would like to acknowledge the constant effort and support of many individuals who made possible the completion of this thesis. My sincerest thanks to Dr. Angelo Miele for his guidance and help. Also, I wish to thank Dr. Richard Tapia and Dr. Enrique Barrera, members of the Thesis Committee, for their advice and support. I thank Powtawche Williams and Marco Ciarcia for being both my colleagues and friends. I also thank my other friends, Eddie Castillo, Edward Gonzales, and Denis Ridzal, for making my experience at Rice University a wonderful one. I thank Dr. Creston King for helping me get into Rice University and being an excellent mentor at Loyola. And of course, my thanks to my family, especially my sister Karla, father William and beloved mother Patricia, for their eternal love and kindness.

Table of Contents

1. Introduction	1
2. Equations of Motion	3
3. Ascending Hohmann Transfer	5
3.1. Remark	6
4. Descending Hohmann Transfer	8
4.1. Remark	9
5. Maximum Path Inclination	10
5.1. Remark	11
6. Dimensionless Speed	12
7. Optimality of the Hohmann Transfer	14
7.1. Proof of Optimality	14
7.2. Remark	17
7.3. Computational Verification	17
8. Applications to Interplanetary Transfer	19
9. Alternative Transfer Maneuvers	22
9.1. Biparabolic Transfer	22
9.2. Bielliptic Transfer	22
9.3. Remark	23
10. Conclusions	24
References	25
List of Tables	27
List of Figures	29
Tables	30
Figures	37

1. Introduction

Walter Hohmann was born in 1880 in the town of Hardheim, near Würzburg, in Germany. He studied civil engineering at the Technical University of Munich achieving the Diploma Degree in 1904. Later on, he continued his studies in civil engineering at the Technical University of Aachen achieving the Doctor Degree in 1919. His lifetime work was in civil engineering, culminating with his appointment as City Architect of the town of Essen in 1912. His lifetime hobby was the study of space maneuvers, culminating with the publication of the book *The Attainability of Celestial Bodies*, published in 1925 (Ref. 1). He died at the end of World War II during a bombing raid on Essen in 1945.

Walter Hohmann worked alone, independently of the considerable German effort on missiles and spacecraft. Perhaps, this is a major reason for the great originality of his work. His most famous study refers to the transfer of a spacecraft from a circular orbit to another circular orbit in a central gravitational field. He concluded that, energetically speaking, the most efficient trajectory is the elliptical trajectory bitangent to the terminal orbits (Ref. 1), which became known as the Hohmann transfer maneuver. With the advent of the space program in 1947, the Hohmann transfer maneuver became the most fundamental maneuver in space (Refs. 2-11).

In this paper, we present a comprehensive study of the Hohmann transfer maneuver. After revisiting its known properties (Sections 2-4), we present a number of supplementary properties which are essential to the qualitative understanding of the Hohmann transfer maneuver (Sections 5-6). Next, we present a simple analytical proof of the optimality of the Hohmann transfer maneuver and we complement it with a

numerical study via the sequential gradient-restoration algorithm for mathematical programming problems (Section 7). Finally, as an application, we present a numerical study of the transfer of a spacecraft from the Earth orbit around the Sun to another planetary orbit around the Sun; we consider both the case of an ascending transfer to the orbits of Mars, Jupiter, Saturn, Uranus, Neptune, and Pluto and the case of a descending transfer to the orbits of Mercury and Venus (Section 8). Next, we discuss alternative modes of transfer such as the biparabolic transfer and bielliptic transfer (Section 9). Finally, we present the conclusions (Section 10).

2. Equations of Motion

We consider the motion of a spacecraft in a central gravitational field. The spacecraft position is determined via the pair (r, θ) , where r is the radial distance from the center of attraction and θ is the phase angle (angle of the radius vector wrt a reference direction). The spacecraft velocity is determined by the pair (V, γ) , where V is the velocity modulus and γ is the angle between the velocity vector and the local horizon (this is perpendicular to the radius vector).

In the absence of aerodynamic and propulsive forces and with reference to the planar case, the equations of motion are

$$\dot{r} = V \sin \gamma, \quad (1a)$$

$$\dot{\theta} = (V / r) \cos \gamma, \quad (1b)$$

$$\dot{V} = -(\mu / r^2) \sin \gamma, \quad (1c)$$

$$\dot{\gamma} = -(\mu / r^2 V) \cos \gamma + (V / r) \cos \gamma, \quad (1d)$$

where the dot denotes derivative with respect to the time t . Let

$$E = V^2 / 2 - \mu / r \quad (2a)$$

denote the total energy (kinetic energy plus potential energy) per unit mass of the spacecraft and let

$$M = rV \cos \gamma \quad (2b)$$

denote the angular momentum of the spacecraft, namely, the moment of the velocity vector with respect to the center of attraction. With this understanding, the equations of motion admit the well-known first integrals

$$E = \text{const}, \quad (3a)$$

$$M = \text{const}, \quad (3b)$$

which are essential to the analysis of a Hohmann transfer.

3. Ascending Hohmann Transfer

We consider the ascending transfer of a spacecraft from a low circular orbit to a high circular orbit under the following assumptions:

- (A1) the low orbit and the high orbit are circular and coplanar;
- (A2) there is only one source of gravitational attraction along the entire trajectory;
- (A3) circularization of the motion is assumed at both the departure and arrival;
- (A4) velocity impulses are applied at only the terminal points of the trajectory and tangentially to the trajectory.

Let the subscripts 0 and 1 denote the spacecraft conditions before and after the application of the accelerating velocity impulse at departure. Let the subscripts 2 and 3 denote the spacecraft conditions before and after the application of the accelerating velocity impulse at arrival. With this understanding, the following relations can be written at the departure:

$$r_1 = r_0, \tag{4a}$$

$$V_1 = V_0 + \Delta V_0, \quad V_0 = \sqrt{\mu / r_0}, \tag{4b}$$

$$\gamma_1 = \gamma_0 = 0, \tag{4c}$$

and at the arrival:

$$r_3 = r_2, \tag{5a}$$

$$V_3 = V_2 + \Delta V_2, \quad V_2 = \sqrt{\mu / r_2}, \tag{5b}$$

$$\gamma_3 = \gamma_2 = 0. \tag{5c}$$

Use of the energy and angular momentum integrals between the points 1 and 2 leads to the supplementary relations

$$V_1^2/2 - \mu/r_1 = V_2^2/2 - \mu/r_2, \quad (6a)$$

$$r_1 V_1 = r_2 V_2. \quad (6b)$$

Equations (4) – (6) admit the following solutions:

$$V_1 = V_0 \sqrt{r_3/r_{\text{ave}}}, \quad V_0 = \sqrt{\mu/r_0}, \quad (7a)$$

$$V_2 = V_3 \sqrt{r_0/r_{\text{ave}}}, \quad V_3 = \sqrt{\mu/r_3}, \quad (7b)$$

in which

$$r_{\text{ave}} = (r_0 + r_3)/2 \quad (7c)$$

denotes the average radius. As a consequence, the velocity impulses at the departure and arrival are given by

$$\Delta V_0 = V_1 - V_0 = V_0 (\sqrt{r_3/r_{\text{ave}}} - 1), \quad (8a)$$

$$\Delta V_2 = V_3 - V_2 = V_3 (1 - \sqrt{r_0/r_{\text{ave}}}). \quad (8b)$$

Also, the values of the energy and angular momentum constants become

$$E_0 = -\mu/2r_0, \quad M_0 = V_0 r_0, \quad (9a)$$

$$E_1 = -\mu/2r_{\text{ave}}, \quad M_1 = V_1 r_0, \quad (9b)$$

$$E_2 = -\mu/2r_{\text{ave}}, \quad M_2 = V_2 r_3, \quad (9c)$$

$$E_3 = -\mu/2r_3, \quad M_3 = V_3 r_3. \quad (9d)$$

3.1. Remark. In polar coordinates, the geometry of the ascending Hohmann transfer is described by the equation

$$r = p/(1 + e \cos \theta), \quad (10a)$$

where p is the parameter, e the eccentricity, and θ the phase angle. In turn, the values of the parameter and eccentricity are given by

$$p = 2r_0r_3/(r_0 + r_3), \quad (10b)$$

$$e = (r_3 - r_0)/(r_0 + r_3). \quad (10c)$$

Other quantities of interest are the phase angle travel of the spacecraft $\theta(\tau) - \theta(0)$, transfer time τ , the characteristic velocity ΔV , and propellant mass ratio m_p/m_0 (ratio of the propellant mass m_p required for transfer to the initial mass of the spacecraft m_0). These quantities are given by the relations

$$\theta(\tau) - \theta(0) = \pi, \quad (11a)$$

$$\tau = \pi \sqrt{r_{\text{ave}}^3/\mu}, \quad r_{\text{ave}} = (r_0 + r_3)/2, \quad (11b)$$

$$\Delta V = \Delta V_0 + \Delta V_2, \quad (11c)$$

$$m_p/m_0 = 1 - \exp(\Delta V/V_e), \quad V_e = g_{\text{SL}} I_{\text{sp}}, \quad (11d)$$

where V_e is the exit velocity (velocity of the jet exiting the rocket engine relative to the spacecraft), I_{sp} is the specific impulse of the rocket engine, and g_{SL} is a reference acceleration (acceleration of gravity at sea level on Earth).

4. Descending Hohmann Transfer

We consider the descending transfer of a spacecraft from a high circular orbit to a low circular orbit under Assumptions (A1) – (A4). Let the subscripts 0 and 1 denote the spacecraft conditions before and after the application of the braking velocity impulse at departure. Let the subscripts 2 and 3 denote the spacecraft conditions before and after the application of the braking velocity impulse at arrival. With this understanding, the following relations can be written at the departure:

$$r_1 = r_0, \quad (12a)$$

$$V_1 = V_0 - \Delta V_0, \quad V_0 = \sqrt{\mu/r_0}, \quad (12b)$$

$$\gamma_1 = \gamma_0 = 0, \quad (12c)$$

and at the arrival:

$$r_3 = r_2, \quad (13a)$$

$$V_3 = V_2 - \Delta V_2, \quad V_2 = \sqrt{\mu/r_2}, \quad (13b)$$

$$\gamma_3 = \gamma_2 = 0. \quad (13c)$$

Use of the energy and angular momentum integrals between the points 1 and 2 leads to the supplementary relations

$$V_1^2/2 - \mu/r_1 = V_2^2/2 - \mu/r_2, \quad (14a)$$

$$r_1 V_1 = r_2 V_2. \quad (14b)$$

Equations (12) – (14) admit the following solutions:

$$V_1 = V_0 \sqrt{r_3/r_{ave}}, \quad V_0 = \sqrt{\mu/r_0}, \quad (15a)$$

$$V_2 = V_3 \sqrt{r_0/r_{ave}}, \quad V_3 = \sqrt{\mu/r_3}, \quad (15b)$$

in which

$$r_{\text{ave}} = (r_0 + r_3)/2 \quad (15c)$$

denotes the average radius. As a consequence, the velocity impulses at the departure and arrival are given by

$$\Delta V_0 = V_0 - V_1 = V_0(1 - \sqrt{r_3/r_{\text{ave}}}), \quad (16a)$$

$$\Delta V_2 = V_2 - V_3 = V_3(\sqrt{r_0/r_{\text{ave}}} - 1). \quad (16b)$$

Also, the values of the energy and angular momentum constants become

$$E_0 = -\mu/2r_0, \quad M_0 = V_0r_0, \quad (17a)$$

$$E_1 = -\mu/2r_{\text{ave}}, \quad M_1 = V_1r_0, \quad (17b)$$

$$E_2 = -\mu/2r_{\text{ave}}, \quad M_2 = V_2r_3, \quad (17c)$$

$$E_3 = -\mu/2r_3, \quad M_3 = V_3r_3. \quad (17d)$$

4.1. Remark. In polar coordinates, the geometry of the descending Hohmann transfer is described by the equation

$$r = p/(1 - e \cos \theta), \quad (18a)$$

where p is the parameter, e the eccentricity, and θ the phase angle. In turn, the values of the parameter and eccentricity are given by

$$p = 2r_0r_3/(r_0 + r_3), \quad (18b)$$

$$e = (r_0 - r_3)/(r_0 + r_3). \quad (18c)$$

The phase angle travel $\theta(\tau) - \theta(0)$, transfer time τ , characteristic velocity ΔV , and propellant mass ratio m_p/m_0 are the same as for ascending transfer and therefore are given by Eqs. (11).

5. Maximum Path Inclination

For the ascending Hohmann transfer, the path inclination γ vanishes at the endpoints and is positive everywhere else. Therefore, there is a point on the Hohmann transfer trajectory where the path inclination γ has a maximum value (Ref. 8).

(i) One way to compute the γ_{\max} point is to make use of the energy and angular momentum integrals, that is, to formulate the following mathematical programming problem in the (r, V, γ) space:

$$\min \quad \cos \gamma, \quad (19a)$$

$$\text{s.t.} \quad V^2 / 2 - \mu / r - E = 0, \quad (19b)$$

$$rV \cos \gamma - M = 0. \quad (19c)$$

This problem has three variables, two constraints, and hence one degree of freedom. Let λ_E and λ_M denote the Lagrange multipliers associated with the energy and angular momentum constraints and let

$$F = \cos \gamma + \lambda_E (V^2 / 2 - \mu / r - E) + \lambda_M (rV \cos \gamma - M) \quad (20)$$

denote the augmented function associated with problem (19). The first-order optimality conditions are

$$F_r = \lambda_E \mu / r^2 + \lambda_M V \cos \gamma = 0, \quad (21a)$$

$$F_V = \lambda_E V + \lambda_M r \cos \gamma = 0, \quad (21b)$$

$$F_\gamma = -(1 + \lambda_M r V) \sin \gamma = 0. \quad (21c)$$

For any given triplet (r, V, γ) , Eqs. (21a) and (21b) are linear and homogeneous in the multipliers λ_E and λ_M . This subsystem admits nontrivial solutions for the multipliers providing its Jacobian determinant vanishes,

$$\begin{vmatrix} \mu/r^2 & V \cos \gamma \\ V & r \cos \gamma \end{vmatrix} = 0, \quad (22a)$$

and this occurs precisely when

$$V = \sqrt{\mu/r}. \quad (22b)$$

The meaning of Eq. (22b) is that, at the γ_{\max} point, the spacecraft velocity equals the local circular velocity. Let the subscript 4 denote the γ_{\max} point. Omitting details for the sake of brevity, use of the energy and angular momentum integrals yields the following values for the radial distance and corresponding velocity

$$r_4 = r_{\text{ave}} = (r_0 + r_3)/2, \quad (22c)$$

$$V_4 = \sqrt{\mu/r_4}. \quad (22d)$$

Therefore, the γ_{\max} point is the midradius point of the Hohmann transfer.

(ii) An alternative way to find the γ_{\max} point is to use the differential system (1), more precisely Eq. (1d). If we set

$$\dot{\gamma} = 0 \quad (23a)$$

in Eq. (1d), we see once more that

$$V = \sqrt{\mu/r}. \quad (23b)$$

5.1. Remark. For the descending Hohmann transfer, the path inclination γ vanishes at the endpoints and is negative everywhere else. Therefore, there is a point on the Hohmann transfer trajectory where the path inclination γ has a minimum value, hence the negative of the path inclination $-\gamma$ has a maximum value.

Proceeding in analogy with (i) and (ii), we conclude that the γ_{\min} point [hence, the $(-\gamma)_{\max}$ point] occurs precisely when the relation (22b) or (23b) is satisfied.

6. Dimensionless Speed

Let V denote the spacecraft velocity, let V_c denote the local circular velocity

$$V_c = \sqrt{\mu/r}, \quad (24a)$$

and let

$$u = V/V_c = V\sqrt{r/\mu}, \quad (24b)$$

denote the ratio of the spacecraft velocity to the local circular velocity (Ref. 8).

Regardless of the value of the path inclination γ , the spacecraft velocity is called circular if $u = 1$, supercircular if $u > 1$, and subcircular if $u < 1$. This terminology allows us to give a simple and elegant interpretation to the Hohmann transfer results, due to the fact that the value $u = 1$ occurs three times: prior to departure (point 0), at midradius (point 4), and after arrival (point 3).

(i) For an ascending Hohmann transfer from a low orbit of radius r_0 to a high orbit of radius $r_3 > r_0$, the dimensionless speed (24b) takes the following values:

$$u_0 = 1, \quad (25a)$$

$$u_1 = \sqrt{r_3/r_{\text{ave}}} > 1, \quad (25b)$$

$$u_4 = 1, \quad (25c)$$

$$u_2 = \sqrt{r_0/r_{\text{ave}}} < 1, \quad (25d)$$

$$u_3 = 1. \quad (25e)$$

Hence, the velocity is circular prior to the departure [see (25a)]; it becomes supercircular because of the accelerating velocity impulse at the departure [see (25b)]; as the spacecraft ascends, the velocity decreases becoming circular again at midradius [see (25c)]; as the spacecraft ascends further, the velocity decreases, becoming subcircular and achieving its lowest value when the spacecraft reaches the high orbit [see (25d)]; at this point, an

accelerating velocity impulse is applied and the velocity becomes circular again at the arrival [see (25e)].

For an example, see Figures 1-2, which refer to the transfer of a spacecraft from the Earth orbit around the Sun to the Mars orbit around the Sun.

(ii) For a descending Hohmann transfer from a high orbit of radius r_0 to a low orbit of radius $r_3 < r_0$, the dimensionless speed (24b) takes the following values:

$$u_0 = 1, \quad (26a)$$

$$u_1 = \sqrt{r_3 / r_{\text{ave}}} < 1, \quad (26b)$$

$$u_4 = 1, \quad (26c)$$

$$u_2 = \sqrt{r_0 / r_{\text{ave}}} > 1, \quad (26d)$$

$$u_3 = 1. \quad (26e)$$

Hence, the velocity is circular prior to the departure [see (26a)]; it becomes subcircular because of the braking velocity impulse at the departure [see (26b)]; as the spacecraft descends, the velocity increases becoming circular again at midradius [see (26c)]; as the spacecraft descends further, the velocity increases, becoming supercircular and achieving its largest value when the spacecraft reaches the low orbit [see (26d)]; at this point, a braking velocity impulse is applied and the velocity becomes circular again at the arrival [see (26e)].

For an example, see Figures 3-4, which refer to the transfer of a spacecraft from the Earth orbit around the Sun to the Venus orbit around the Sun.

7. Optimality of the Hohmann Transfer

The equations of the ascending Hohmann transfer (Section 3) were obtained assuming that the velocity impulses at the departure and arrival are applied tangentially to the terminal orbits, which are circular. In other words, the terminal values of the path inclinations are $\gamma_0 = \gamma_1 = \gamma_2 = \gamma_3 = 0$. This reduces the computation of the velocities (7) and hence the computation of the velocity impulses (8) to a feasibility problem.

To establish the optimality of the Hohmann transfer, it is necessary to enlarge the class of trajectories being investigated by assuming that the velocity impulses at the departure and arrival are not necessarily tangential. This is the same as assuming the presence of discontinuities in the path inclination at the departure (from $\gamma_0 = 0$ to $\gamma_1 \neq 0$) and at the arrival (from $\gamma_2 \neq 0$ to $\gamma_3 = 0$).

7.1. Proof of Optimality. Let us decompose the vectorial velocity impulse at the departure into a transversal component ΔV_{0T} and radial component ΔV_{0R} . Analogously, let us decompose the vectorial velocity impulse at the arrival into a transversal component ΔV_{2T} and radial component ΔV_{2R} . These quantities are related to the spacecraft velocity and path inclination (before and after application of the velocity impulses) via the expressions

$$\Delta V_{0T} = V_1 \cos \gamma_1 - V_0, \quad \Delta V_{0R} = V_1 \sin \gamma_1 - 0, \quad (27a)$$

$$\Delta V_{2T} = V_3 - V_2 \cos \gamma_3, \quad \Delta V_{2R} = 0 - V_2 \sin \gamma_2. \quad (27b)$$

As a consequence, the moduli of the velocity impulses ΔV_0 and ΔV_1 are given by

$$\Delta V_0 = \sqrt{(V_1 \cos \gamma_1 - V_0)^2 + (V_1 \sin \gamma_1)^2}, \quad (28a)$$

$$\Delta V_2 = \sqrt{(V_3 - V_2 \cos \gamma_2)^2 + (V_2 \sin \gamma_2)^2}, \quad (28b)$$

which can be rewritten as

$$\Delta V_0 = \sqrt{(V_1 - V_0)^2 + 2V_0V_1(1 - \cos \gamma_1)}, \quad (29a)$$

$$\Delta V_2 = \sqrt{(V_3 - V_2)^2 + 2V_2V_3(1 - \cos \gamma_2)}, \quad (29b)$$

while the total characteristic velocity (total velocity impulse) is given by

$$\Delta V = \Delta V_0 + \Delta V_2. \quad (29c)$$

In Eqs. (29), the circular velocities V_0 and V_3 are known quantities. On the other hand, the velocities V_1 , V_2 and path inclinations γ_1 , γ_2 are unknown quantities, which must be consistent with the energy and angular momentum integrals. If these relations are exploited, the problem of minimizing the total characteristic velocity (29) can be formulated as follows:

$$\min \quad \Delta V = \Delta V_0 + \Delta V_2, \quad (30a)$$

$$\Delta V_0 = \sqrt{(V_1 - V_0)^2 + 2V_0V_1(1 - \cos \gamma_1)}, \quad (30b)$$

$$\Delta V_2 = \sqrt{(V_3 - V_2)^2 + 2V_2V_3(1 - \cos \gamma_2)} \quad (30c)$$

$$\text{s.t.} \quad V_1^2 - V_2^2 + 2(V_3^2 - V_0^2) = 0, \quad (30d)$$

$$V_3^2V_1 \cos \gamma_1 - V_0^2V_2 \cos \gamma_2 = 0, \quad (30e)$$

where (30d) is an alternative form of the energy relation and (30e) is an alternative form of the angular momentum relation.

This problem has four variables (V_1 , V_2 , γ_1 , γ_2), two constraints, and hence two degrees of freedom. Let λ_E and λ_M denote the Lagrange multipliers associated with the energy and angular momentum constraints and let

$$\begin{aligned}
F = & \Delta V_0(V_1, \gamma_1) + \Delta V_2(V_2, \gamma_2) \\
& + \lambda_E [V_1^2 - V_2^2 + 2(V_3^2 - V_0^2)] + \lambda_M (V_3^2 V_1 \cos \gamma_1 - V_0^2 V_2 \cos \gamma_2)
\end{aligned} \tag{31}$$

denote the augmented function associated with problem (30). The first - order optimality conditions are

$$\partial F / \partial \gamma_1 = 0, \tag{32a}$$

$$\partial F / \partial \gamma_2 = 0, \tag{32b}$$

$$\partial F / \partial V_1 = 0, \tag{32c}$$

$$\partial F / \partial V_2 = 0. \tag{32d}$$

In particular, (32a) and (32b) yield the result

$$\sin \gamma_1 = 0, \tag{33a}$$

$$\sin \gamma_2 = 0, \tag{33b}$$

implying that

$$\gamma_1 = 0, \tag{34a}$$

$$\gamma_2 = 0. \tag{34b}$$

To sum up, this simple yet rigorous proof allows us to conclude that, to minimize the total characteristic velocity (hence to minimize the mass of propellant consumed), the spacecraft must depart tangentially from the low circular orbit as well as arrive tangentially to the high circular orbit.

With the terminal values of the path inclination known, solution of the feasibility equations (30d) - (30e) yields the unknown velocities,

$$V_1 = V_0 \sqrt{2V_0^2 / (V_0^2 + V_3^2)}, \tag{35a}$$

$$V_2 = V_3 \sqrt{2V_3^2 / (V_0^2 + V_3^2)}, \tag{35b}$$

which can be converted into (15) via simple transformations. Finally, solution of (32c) - (32d) yields the multipliers λ_E and λ_M . The details are omitted for brevity.

For alternative proofs, albeit more complicated proofs, see Refs. 12-14.

7.2. Remark. While the results (34) have been established for an ascending transfer, the same results (34) can be established for a descending transfer. The details are omitted for the sake of brevity.

7.3. Computational Verification. For specific examples, a computational verification of the optimality of the Hohmann transfer can be made using the sequential gradient – restoration algorithm for mathematical programming problems (SGRA, Ref. 15). Two examples are considered.

Earth/Mars Transfer. The first example deals with the ascending transfer of a spacecraft from the Earth orbit (radius r_0) around the Sun to the Mars orbit (radius r_3) around the Sun under the assumption that the Sun is the only source of gravitational attraction. In this example, the Sun gravitational constant is

$$\mu = 1.327 \text{ E11 km}^3/\text{s}^2, \quad (36a)$$

the radii of the terminal orbits are

$$r_0 = 1.496 \text{ E08 km}, \quad r_3 = 2.279 \text{ E08 km}, \quad (36b)$$

and the corresponding terminal velocities are

$$V_0 = 29.78 \text{ km/s}, \quad V_3 = 24.13 \text{ km/s}. \quad (36c)$$

For the Hohmann transfer, the predicted accelerating velocity impulses are

$$\Delta V_0 = 2.945 \text{ km/s}, \quad \Delta V_2 = 2.649 \text{ km/s}, \quad (37a)$$

so that the total characteristic velocity is

$$\Delta V = 5.594 \text{ km/s}. \quad (37b)$$

Earth/Venus Transfer. The second example deals with the descending transfer of a spacecraft from the Earth orbit (radius r_0) around the Sun to the Venus orbit (radius r_3) around the Sun under the assumption that the Sun is the only source of gravitational attraction. In this example, the Sun gravitational constant is

$$\mu = 1.327 \text{ E11 km}^3/\text{s}^2, \quad (38a)$$

the radii of the terminal orbits are

$$r_0 = 1.496 \text{ E08 km}, \quad r_3 = 1.082 \text{ E08 km}, \quad (38b)$$

and the corresponding terminal velocities are

$$V_0 = 29.78 \text{ km/s}, \quad V_3 = 35.02 \text{ km/s}. \quad (38c)$$

For the Hohmann transfer, the predicted braking velocity impulses are

$$\Delta V_0 = 2.496 \text{ km/s}, \quad \Delta V_2 = 2.707 \text{ km/s}, \quad (39a)$$

so that the total characteristic velocity is

$$\Delta V = 5.203 \text{ km/s}. \quad (39b)$$

Results. Computer runs were made for various starting combinations of the departing pair (V_1, γ_1) resulting in the arrival velocity pair (V_2, γ_2) . For both Earth/Mars ascending transfer and Earth/Venus descending transfer, SGRA led to vanishing values of γ_1 and γ_2 (hence vanishing values of the radial velocity impulses ΔV_{0R} and ΔV_{2R}), so that the terminal velocity impulses ΔV_0 and ΔV_2 became identical with their tangential counterpart ΔV_{0T} and ΔV_{2T} . Also, the values achieved for the terminal velocity impulses ΔV_0 and ΔV_2 as well as the total characteristic velocity ΔV were quite close to the values (37) for Earth/Mars transfer and the values (39) for Earth/Venus transfer.

8. Applications to Interplanetary Transfer

In this section, we present results on the interplanetary transfer of a spacecraft from the Earth orbit around the Sun to the orbit of any other planet around the Sun. We include two cases of descending transfer (from Earth orbit to the orbits of Mercury and Venus) and six cases of ascending transfer (from Earth orbit to the orbits of Mars, Jupiter, Saturn, Uranus, Neptune, and Pluto).

Planetary Data. Table 1 shows some basic planetary data. These include average radial distance of planet from Sun r , average velocity V , energy per unit mass E , and angular momentum M (Table 1a) as well as planet mass m , gravitational constant μ , orbital period T , and angular velocity around the Sun ω (Table 1b).

Descending Hohmann Transfer. Tables 2 – 3 refer to the descending Hohmann transfer from Earth orbit to the orbits of Mercury (Table 2) and Venus (Table 3). Tables 2a and 3a contain general properties, namely: velocity impulse at departure ΔV_0 , velocity impulse at arrival ΔV_2 , total characteristic velocity ΔV , and transfer time τ . For interception problems, another quantity of interest is the phase angle difference at departure,

$$\Delta\theta(0) = \theta_M(0) - \theta_E(0) = \pi(1 - \omega_M \tau), \quad \text{Earth/Mars transfer,} \quad (40a)$$

$$\Delta\theta(0) = \theta_V(0) - \theta_E(0) = \pi(1 - \omega_V \tau), \quad \text{Earth/ Venus transfer.} \quad (40b)$$

The above phase angle differences reoccur in time after a synodic period, which is given by

$$T_{\text{syn}} = 2\pi/(\omega_E - \omega_M) = T_E T_M / (T_M - T_E), \quad \text{Earth/Mars transfer,} \quad (41a)$$

$$T_{\text{syn}} = 2\pi/(\omega_V - \omega_E) = T_E T_V / (T_E - T_V), \quad \text{Earth/Venus transfer.} \quad (41b)$$

Tables 2b and 3b show the values of the spacecraft velocity V , radial distance r , energy per unit mass E , and angular momentum M at the four critical points of the transfer, namely:

point 0,	departure,	condition before velocity impulse,
point 1,	departure,	condition after velocity impulse,
point 2,	arrival,	condition before velocity impulse,
point 3,	arrival,	condition after velocity impulse.

Ascending Hohmann Transfer. Tables 4–9 refer to the ascending Hohmann transfer from Earth orbit to the orbits of Mars (Table 4), Jupiter (Table 5), Saturn (Table 6), Uranus (Table 7), Neptune (Table 8), and Pluto (Table 9). These tables are constructed in the same way as Tables 2–3.

Propellant Consumption. The propellant consumed in a Hohmann transfer can be computed with the relation

$$m_p/m_0 = 1 - \exp(-\Delta V/V_e), \quad V_e = g_{SL} I_{sp}. \quad (42)$$

Here, m_p is the propellant consumed, m_0 is the initial mass of the spacecraft, ΔV is the total characteristic velocity, V_e is the velocity of the jet exiting the rocket engine (relative to the spacecraft), g_{SL} is a reference acceleration (acceleration of gravity at sea level on Earth), and I_{sp} is the specific impulse of the rocket engine.

The values of the ratio m_p/m_0 are given in Table 10 for three values of the engine specific impulse, namely:

$$I_{sp} = 450s, \quad \text{hence } V_e = 4.414 \text{ km/s}, \quad (43a)$$

$$I_{sp} = 3000s, \quad \text{hence } V_e = 29.43 \text{ km/s}, \quad (43b)$$

$$I_{sp} = 6000s, \quad \text{hence } V_e = 58.86 \text{ km/s}. \quad (43c)$$

The values (43a) characterize a present-day chemical engine (Space Shuttle). The values (43b) characterize an existing electrical engine (Deep Space One spacecraft). The values (43c) characterize a future electrical engine, already tested at NASA Glenn Space Center in Cleveland, Ohio (Project Prometheus).

If instead of circularizing the motion in the target orbit, we are interested in a planetary flyby, then Eq. (42) must be replaced by

$$m_p/m_0 = 1 - \exp(-\Delta V_0/V_e), \quad V_e = g_{SL} I_{sp}. \quad (44)$$

The values of the above ratio are given in Table 11 for three values of the engine specific impulse, namely, the values (43).

From Tables 10-11, it is clear that the degree of difficulty associated with reaching Mars and Venus (the planets closer to Earth) is much less than that associated with reaching Mercury and the outer planets (Jupiter, Saturn, Uranus, Neptune, and Pluto). See also Table 12 (in two parts), which contains a summary of the general properties.

9. Alternative Transfer Maneuvers

During the early years of the space program, attention was given to transfer maneuvers alternative to the Hohmann transfer maneuver (Fig. 5). These include the biparabolic transfer (Fig. 6) and the bielliptic transfer (Fig. 7).

9.1. Biparabolic Transfer. We refer to the ascending transfer from r_0 to r_3 with $r_3 > r_0$. The biparabolic transfer consists of two branches: (a) a parabolic branch tangent to the departure orbit and going to infinity; (b) a parabolic branch returning from infinity and tangent to the arrival orbit. Because of (a), the velocity V_1 must equal the escape velocity at the radius $r_1 = r_0$; because of (b), the velocity V_2 must equal the escape velocity at the radius $r_2 = r_3$. Hence, the velocity impulse associated with (a) is accelerating, while the velocity impulse associated with (b) is braking. Of course, a third velocity impulse is needed to switch from the parabolic ascending branch to the parabolic descending branch. This third velocity impulse has zero magnitude if the switch is done at infinity; it has a finite magnitude if the switch is done at a finite radius.

The analyses made (Ref. 4) have shown that the total characteristic velocity of the biparabolic transfer is less than that of the Hohmann transfer if $r_3/r_0 > 11.94$. While this result has mathematical interest, it has no practical significance, since a biparabolic transfer requires an infinite time.

9.2. Bielliptic Transfer. Again, we refer to the ascending transfer from r_0 to r_3 with $r_3 > r_0$. The bielliptic transfer consists of two branches: (a) an elliptic branch tangent to the departure orbit; (b) another elliptic branch tangent to the arrival orbit. In turn, the two elliptic branches are tangent to one another at the point where the switch is

made. This type of transfer requires three velocity impulses: at departure, at arrival, and at the switch point from the first ellipse to the second ellipse.

The analyses made (Ref. 4) have shown that the total characteristic velocity of the bielliptic transfer is less than that of the Hohmann transfer in the range $11.94 \leq r_3/r_0 \leq 15.58$, providing the switch from the first ellipse to the second ellipse occurs at a radius sufficiently large. For $r_3/r_0 \geq 15.58$, the bielliptic transfer is always more economical than the Hohmann transfer providing the midcourse impulse occurs outside the arrival orbit ($r > r_3$). These advantages are obtained at a price: an increase of the transfer time, which in some cases might be double that of the Hohmann transfer.

9.3. Remark. If we require the spacecraft to move in the region of space bounded by the terminal orbits, namely if

$$r_0 \leq r \leq r_3, \quad \text{ascending transfer,} \quad (47)$$

then the solution of minimum total characteristic velocity is once more the Hohmann transfer, regardless of the value of the ratio r_3/r_0 . In effect, inequality (47) rules out the possibility of either a biparabolic solution or a bielliptic solution, since each of these solutions requires the spacecraft to travel outside the region of space bounded by the terminal orbits.

10. Conclusions

We present a complete study of the Hohmann transfer maneuver between two circular coplanar orbits. Starting from basic orbital mechanics, a complete description of the maneuver is given for both the case of an ascending transfer and the case of a descending transfer. We include a number of supplementary properties of the Hohmann transfer. Specifically, the path inclination is maximum at midradius and at this point the spacecraft velocity equals the local circular velocity. This implies that the spacecraft velocity equals the local circular velocity three times along a Hohmann transfer trajectory: before departure, at midradius, and after arrival. In turn, this allows us to subdivide the trajectory into a region where the velocity is supercircular and a region where the velocity is subcircular: for ascending transfer, the supercircular region precedes the subcircular region; for descending transfer, the opposite occurs.

We present a simple yet rigorous analytical proof of the optimality of the Hohmann transfer. Rather than using a geometric argument, as previously done, the proof is done via mathematical programming techniques. We complement the analytical proof with a numerical study via the sequential gradient-restoration algorithm. Finally, as an application, we present a numerical study of the transfer of a spacecraft from the Earth orbit around the Sun to another planetary orbit around the Sun for both the case of an ascending transfer (orbits of Mars, Jupiter, Saturn, Uranus, Neptune, and Pluto) and the case of a descending transfer (orbits of Mercury and Venus).

References

1. HOHMANN, W., *The Attainability of Celestial Bodies*, R. Oldenbourg Verlag, Munich, Germany, 1925 (in German); see also NASA Technical Translation F-44, Washington, DC, 1960 (in English).
2. MAREC, J.P., *Optimal Space Trajectories*, Studies in Astronautics, Elsevier, Amsterdam, Holland, Vol. 1, 1979.
3. LAWDEN, D. F., *Optimal Transfers between Coplanar Elliptical Orbits*, Journal of Guidance, Control, and Dynamics, Vol. 15, No. 3, pp. 788-791, 1991.
4. PRUSSING, J. E., and CONWAY, B. A., *Orbital Mechanics*, Oxford University Press, Oxford, UK, 1993.
5. BATTIN, R. H., *An Introduction to the Mathematics and Methods of Astrodynamics*, Revised Edition, American Institute of Aeronautics and Astronautics, Reston, Virginia, 1999.
6. CHOBOTOV, V.A., *Orbital Mechanics*, 3rd Edition, American Institute of Aeronautics and Astronautics, Reston, Virginia, 2002.
7. MIELE, A., and WANG, T., *General Solution for the Optimal Trajectory of an AFE-Type Spacecraft*, Acta Astronautica, Vol. 26, No. 12, pp. 855-866, 1992.
8. MIELE, A., *Recent Advances in the Optimization and Guidance of Aeroassisted Orbital Transfers*, The 1st John V. Breakwell Memorial Lecture, Acta Astronautica, Vol. 38, No.10, pp. 747-768, 1996.
9. MIELE, A., and WANG, T., *Optimal Transfers from an Earth Orbit to a Mars Orbit*, Acta Astronautica, Vol. 45, No. 3, pp. 119-113, 1999.

10. MIELE, A., and WANG, T., *Optimal Trajectories and Mirror Properties for Round-Trip Mars Missions*, Acta Astronautica, Vol. 45, No. 11, pp. 655-668, 1999.
11. MIELE, A., WANG, T., and MANCUSO, S., *Optimal Free-Return Trajectories for Moon Missions and Mars Missions*, Journal of the Astronautical Sciences, Vol. 48, Nos. 2-3, pp. 183-206, 2000.
12. TING, L., *Optimum Orbital Transfer by Several Impulses*, Acta Astronautica, Vol. 6, No. 5, pp. 256-265, 1960.
13. BARRAR, R.B., *An Analytic Proof That the Hohmann-Type Transfer is the True Minimum Two-Impulse Transfer*, Acta Astronautica, Vol. 9, No. 1, pp. 1-11, 1963.
14. PALMORE, J., *An Elementary Proof of the Optimality of Hohmann Transfers*, Journal of Guidance, Control, and Dynamics, Vol. 7, No. 5, pp. 629-630, 1984.
15. MIELE, A., HUANG, H.Y., and HEIDEMAN, J.C., *Sequential Gradient – Restoration Algorithm for the Minimization of Constrained Functions: Ordinary and Conjugate Gradient Versions*, Journal of Optimization Theory and Applications, Vol. 4, No. 4, pp. 213-243, 1964.

List of Tables

Table 1a. Planetary data

Table 1b. Planetary data (continued)

Table 2a. Earth orbit to Mercury orbit,
descending Hohmann transfer, general properties.

Table 2b. Earth orbit to Mercury orbit,
descending Hohmann transfer, detailed properties.

Table 3a. Earth orbit to Venus orbit,
descending Hohmann transfer, general properties.

Table 3b. Earth orbit to Venus orbit,
descending Hohmann transfer, detailed properties.

Table 4a. Earth orbit to Mars orbit,
ascending Hohmann transfer, general properties.

Table 4b. Earth orbit to Mars orbit,
ascending Hohmann transfer, detailed properties.

Table 5a. Earth orbit to Jupiter orbit,
ascending Hohmann transfer, general properties.

Table 5b. Earth orbit to Jupiter orbit,
ascending Hohmann transfer, detailed properties.

Table 6a. Earth orbit to Saturn orbit,
ascending Hohmann transfer, general properties.

Table 6b. Earth orbit to Saturn orbit,
ascending Hohmann transfer, detailed properties.

- Table 7a. Earth orbit to Uranus orbit,
ascending Hohmann transfer, general properties.
- Table 7b. Earth orbit to Uranus orbit,
ascending Hohmann transfer, detailed properties.
- Table 8a. Earth orbit to Neptune orbit,
ascending Hohmann transfer, general properties.
- Table 8b. Earth orbit to Neptune orbit,
ascending Hohmann transfer, detailed properties.
- Table 9a. Earth orbit to Pluto orbit,
ascending Hohmann transfer, general properties.
- Table 9b. Earth orbit to Pluto orbit,
ascending Hohmann transfer, detailed properties.
- Table 10. Propellant mass ratio m_p/m_0 for Earth-to-Planet transfer (circularization of motion).
- Table 11. Propellant mass ratio m_p/m_0 for Earth-to-Planet flyby.
- Table 12a. Earth-to-Planet Transfer:
Summary of general properties.
- Table 12b. Earth-to-Planet Transfer:
Summary of general properties.

List of Figures

- Fig. 1. Earth orbit to Mars orbit transfer:
Velocity vs radial distance.
- Fig. 2. Earth orbit to Mars orbit transfer:
Path inclination vs radial distance.
- Fig. 3. Earth orbit to Venus orbit transfer:
Velocity vs radial distance
- Fig. 4. Earth orbit to Venus orbit transfer:
Path inclination vs radial distance
- Fig. 5. Hohmann transfer: Ascending case
- Fig. 6. Bielliptic transfer: Ascending case
- Fig. 7. Biparabolic transfer: Ascending case

Table 1a. Planetary data.

	r [km]	V [km/s]	E [km ² /s ²]	M [km ² /s]
Mercury	0.579×10^8	47.873	-1145.90	2.772×10^9
Venus	1.082×10^8	35.023	-613.30	3.789×10^9
Earth	1.496×10^8	29.785	-443.58	4.456×10^9
Mars	2.279×10^8	24.130	-291.12	5.500×10^9
Jupiter	7.783×10^8	13.058	-85.26	10.164×10^9
Saturn	14.294×10^8	9.636	-46.42	13.773×10^9
Uranus	28.710×10^8	6.799	-23.11	19.520×10^9
Neptune	45.043×10^8	5.428	-14.73	24.450×10^9
Pluto	59.135×10^8	4.737	-11.22	28.015×10^9

Table 1b. Planetary data (continued).

	m [kg]	μ [km ³ /s ²]	T [days]	ω [deg/day]
Mercury	3.303×10^{23}	2.204×10^4	87.969	4.092×10^0
Venus	4.869×10^{24}	3.249×10^5	224.701	1.602×10^0
Earth	5.976×10^{24}	3.987×10^5	365.256	9.856×10^{-1}
Mars	6.421×10^{23}	4.285×10^4	686.986	5.240×10^{-1}
Jupiter	1.900×10^{27}	1.268×10^8	4332.66	8.309×10^{-2}
Saturn	5.688×10^{26}	3.795×10^7	10759.4	3.346×10^{-2}
Uranus	8.686×10^{25}	5.796×10^6	30688.9	1.173×10^{-2}
Neptune	1.024×10^{26}	6.833×10^6	60132.3	5.987×10^{-3}
Pluto	1.290×10^{22}	8.608×10^2	90467.2	3.979×10^{-3}
Sun	1.989×10^{30}	1.327×10^{11}		
Universal gravitational constant $G = 6.67259 \times 10^{-20}$ [km ³ /kg s ²].				

Table 2a. Earth orbit to Mercury orbit,
descending Hohmann transfer, general properties.

ΔV_0 [km/s]	ΔV_2 [km/s]	ΔV [km/s]	τ [days]	$\Delta\theta(0)$ [deg]	T_{syn} [days]
7.533	9.611	17.144	94.63	-207.24	115.88

Table 2b. Earth orbit to Mercury orbit,
descending Hohmann transfer, detailed properties.

Point	Orbit	r [km]	V [km/s]	E [km ² /s ²]	M [km ² /s]
0	HSO(-)	1.496×10^8	29.785	-443.58	4.456×10^9
1	HSO(+)	1.496×10^8	22.252	-639.58	3.329×10^9
2	LSO(-)	0.579×10^8	57.484	-639.58	3.329×10^9
3	LSO(+)	0.579×10^8	47.873	-1145.90	2.772×10^9

Table 3a. Earth orbit to Venus orbit,
descending Hohmann transfer, general properties.

ΔV_0 [km/s]	ΔV_2 [km/s]	ΔV [km/s]	τ [days]	$\Delta\theta(0)$ [deg]	T_{syn} [days]
2.496	2.707	5.203	144.17	-51.01	583.96

Table 3b. Earth orbit to Venus orbit,
descending Hohmann transfer, detailed properties.

Point	Orbit	r [km]	V [km/s]	E [km ² /s ²]	M [km ² /s]
0	HSO(-)	1.496×10^8	29.785	-443.58	4.456×10^9
1	HSO(+)	1.496×10^8	27.289	-514.81	4.082×10^9
2	LSO(-)	1.082×10^8	37.730	-514.81	4.082×10^9
3	LSO(+)	1.082×10^8	35.023	-613.30	3.789×10^9

Table 4a. Earth orbit to Mars orbit,
ascending Hohmann transfer, general properties.

ΔV_0 [km/s]	ΔV_2 [km/s]	ΔV [km/s]	τ [days]	$\Delta\theta(0)$ [deg]	T_{syn} [days]
2.945	2.649	5.594	253.23	47.30	779.87

Table 4b. Earth orbit to Mars orbit,
ascending Hohmann transfer, detailed properties.

Point	Orbit	r [km]	V [km/s]	E [km ² /s ²]	M [km ² /s]
0	HSO(-)	1.496×10^8	29.785	-443.58	4.456×10^9
1	HSO(+)	1.496×10^8	32.730	-351.53	4.896×10^9
2	LSO(-)	2.279×10^8	21.481	-351.53	4.896×10^9
3	LSO(+)	2.279×10^8	24.130	-291.12	5.500×10^9

Table 5a. Earth orbit to Jupiter orbit,
ascending Hohmann transfer, general properties.

ΔV_0 [km/s]	ΔV_2 [km/s]	ΔV [km/s]	τ [days]	$\Delta\theta(0)$ [deg]	T_{syn} [days]
8.793	5.643	14.436	733.60	119.07	398.87

Table 5b. Earth orbit to Jupiter orbit,
ascending Hohmann transfer, detailed properties.

Point	Orbit	r [km]	V [km/s]	E [km ² /s ²]	M [km ² /s]
0	HSO(-)	1.496×10^8	29.785	-443.58	4.456×10^9
1	HSO(+)	1.496×10^8	38.578	-143.03	5.771×10^9
2	LSO(-)	7.783×10^8	7.415	-143.03	5.771×10^9
3	LSO(+)	7.783×10^8	13.058	-85.26	10.163×10^9

Table 6a. Earth orbit to Saturn orbit,
ascending Hohmann transfer, general properties.

ΔV_0 [km/s]	ΔV_2 [km/s]	ΔV [km/s]	τ [days]	$\Delta\theta(0)$ [deg]	T_{syn} [days]
10.292	5.441	15.734	1296.84	136.72	378.08

Table 6b. Earth orbit to Saturn orbit,
ascending Hohmann transfer, detailed properties.

Point	Orbit	r [km]	V [km/s]	E [km ² /s ²]	M [km ² /s]
0	HSO(-)	1.496×10^8	29.785	-443.58	4.456×10^9
1	HSO(+)	1.496×10^8	40.078	-84.05	5.996×10^9
2	LSO(-)	14.294×10^8	4.194	-84.05	5.996×10^9
3	LSO(+)	14.294×10^8	9.636	-46.42	13.773×10^9

Table 7a. Earth orbit to Uranus orbit,
ascending Hohmann transfer, general properties.

ΔV_0 [km/s]	ΔV_2 [km/s]	ΔV [km/s]	τ [days]	$\Delta\theta(0)$ [deg]	T_{syn} [days]
11.281	4.659	15.940	2542.03	150.20	369.64

Table 7b. Earth orbit to Uranus orbit,
ascending Hohmann transfer, detailed properties.

Point	Orbit	r [km]	V [km/s]	E [km ² /s ²]	M [km ² /s]
0	HSO(-)	1.496×10^8	29.785	-443.58	4.456×10^9
1	HSO(+)	1.496×10^8	41.066	-43.94	6.143×10^9
2	LSO(-)	28.710×10^8	2.140	-43.94	6.143×10^9
3	LSO(+)	28.710×10^8	6.799	-23.11	19.520×10^9

Table 8a. Earth orbit to Neptune orbit,
ascending Hohmann transfer, general properties.

ΔV_0 [km/s]	ΔV_2 [km/s]	ΔV [km/s]	τ [days]	$\Delta\theta(0)$ [deg]	T_{syn} [days]
11.655	4.052	15.707	3952.22	156.42	367.47

Table 8b. Earth orbit to Neptune orbit,
ascending Hohmann transfer, detailed properties.

Point	Orbit	r [km]	V [km/s]	E [km ² /s ²]	M [km ² /s]
0	HSO(-)	1.496×10^8	29.785	-443.58	4.456×10^9
1	HSO(+)	1.496×10^8	41.440	-28.52	6.199×10^9
2	LSO(-)	45.043×10^8	1.376	-28.52	6.199×10^9
3	LSO(+)	45.043×10^8	5.428	-14.73	24.451×10^9

Table 9a. Earth orbit to Pluto orbit,
ascending Hohmann transfer, general properties.

ΔV_0 [km/s]	ΔV_2 [km/s]	ΔV [km/s]	τ [days]	$\Delta\theta(0)$ [deg]	T_{syn} [days]
11.815	3.685	15.41	5168.81	159.50	366.72

Table 9b. Earth orbit to Pluto orbit,
ascending Hohmann transfer, detailed properties.

Point	Orbit	r [km]	V [km/s]	E [km ² /s ²]	M [km ² /s]
0	HSO(-)	1.496×10^8	29.785	-443.58	4.456×10^9
1	HSO(+)	1.496×10^8	41.599	-21.89	6.223×10^9
2	LSO(-)	59.135×10^8	1.052	-21.89	6.223×10^9
3	LSO(+)	59.135×10^8	4.737	-11.22	28.015×10^9

Table 10. Propellant mass ratio m_p/m_0 for Earth-to-Planet transfer (circularization of motion).

	$I_{sp} = 450[s]$	$I_{sp} = 3000[s]$	$I_{sp} = 6000[s]$
Mercury	0.9794	0.4415	0.2527
Venus	0.6923	0.1621	0.0846
Earth	0.0000	0.0000	0.0000
Mars	0.7185	0.1731	0.0907
Jupiter	0.9620	0.3877	0.2175
Saturn	0.9717	0.4141	0.2346
Uranus	0.9730	0.4182	0.2372
Neptune	0.9715	0.4136	0.2342
Pluto	0.9701	0.4094	0.2315

Table 11. Propellant mass ratio m_p/m_0 for Earth-to-Planet flyby.

	$I_{sp} = 450[s]$	$I_{sp} = 3000[s]$	$I_{sp} = 6000[s]$
Mercury	0.8185	0.2258	0.1201
Venus	0.4319	0.0813	0.0415
Earth	0.0000	0.0000	0.0000
Mars	0.4868	0.0952	0.0488
Jupiter	0.8636	0.2583	0.1388
Saturn	0.9029	0.2951	0.1604
Uranus	0.9223	0.3184	0.1744
Neptune	0.9287	0.3270	0.1796
Pluto	0.9312	0.3307	0.1819

Table 12a. Earth-to-Planet Transfer:
Summary of general properties.

	ΔV_0 [km/s]	ΔV_2 [km/s]	ΔV [km/s]
Mercury	7.533	9.611	14.144
Venus	2.496	2.707	5.203
Earth	0.000	0.000	0.000
Mars	2.945	2.649	5.594
Jupiter	8.793	5.634	14.436
Saturn	10.292	5.441	15.734
Uranus	11.281	4.659	15.940
Neptune	11.655	4.052	15.707
Pluto	11.815	3.685	15.410

Table 12b. Earth-to-Planet Transfer:
Summary of general properties.

	τ [days]	$\Delta\theta(0)$ [deg]	T_{syn} [days]
Mercury	94.63	-207.24	115.88
Venus	144.17	-51.01	583.96
Earth	0.00	0.00	0.00
Mars	253.23	47.30	779.87
Jupiter	733.60	119.07	398.87
Saturn	1296.84	136.72	378.08
Uranus	2542.03	150.20	369.64
Neptune	3952.22	156.42	367.47
Pluto	5168.81	159.50	366.72

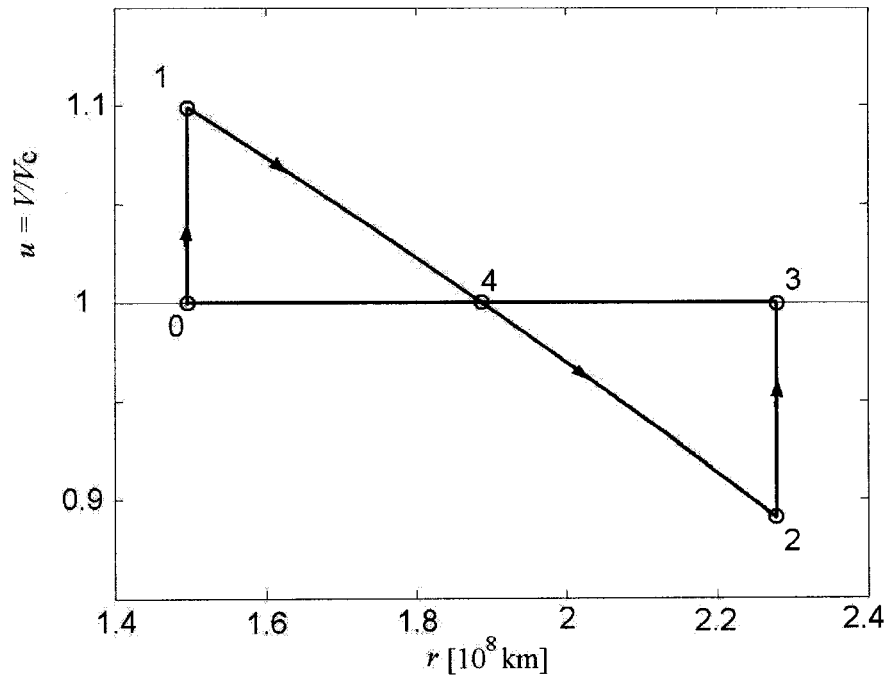


Fig. 1. Earth orbit to Mars orbit transfer:
Velocity vs radial distance.

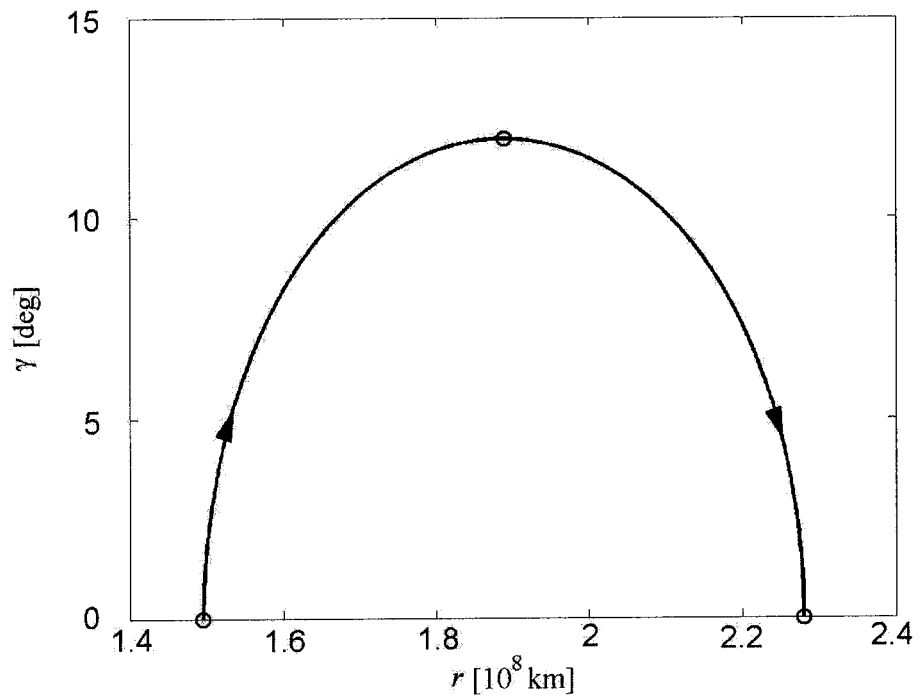


Fig. 2. Earth orbit to Mars orbit transfer:
Path inclination vs radial distance.

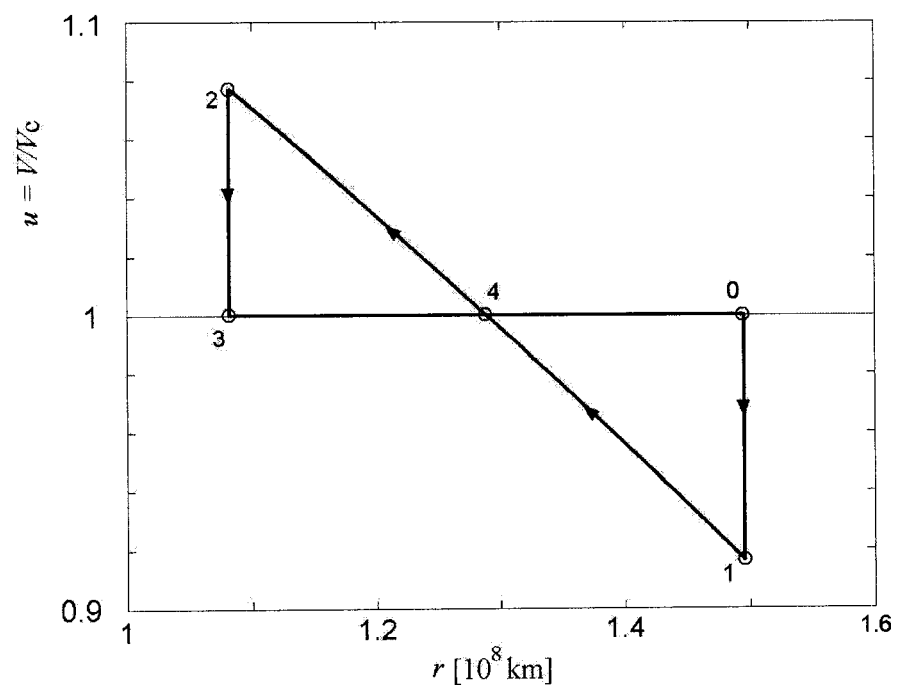


Fig. 3. Earth orbit to Venus orbit transfer:
Velocity vs radial distance.

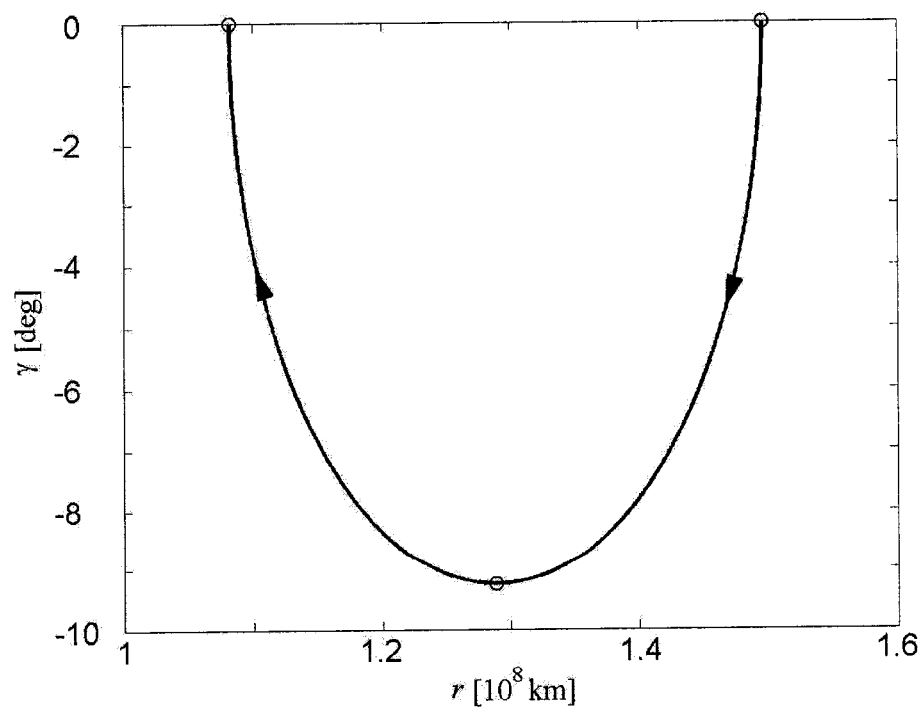


Fig. 4. Earth orbit to Venus orbit transfer:
Path inclination vs radial distance.

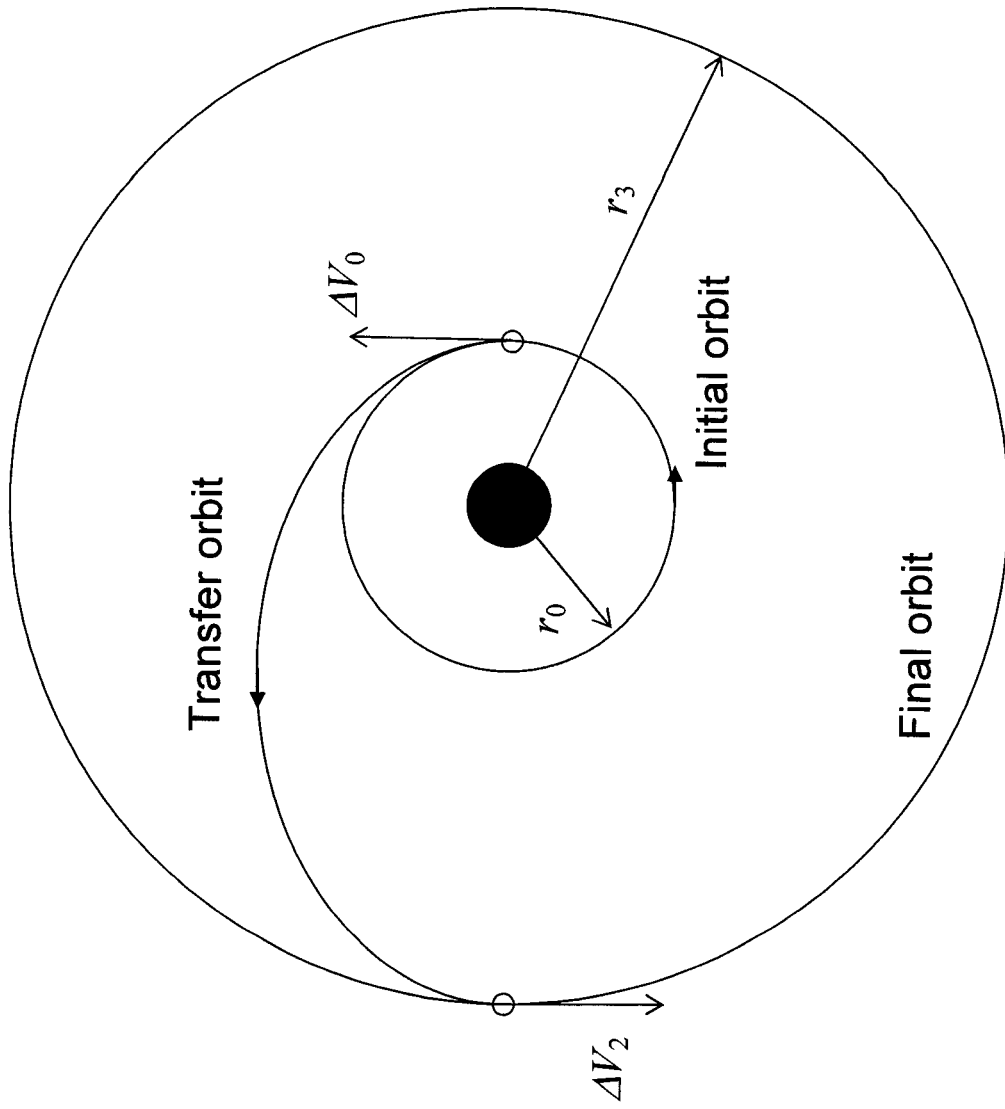


Fig. 5. Hohmann transfer: Ascending case.

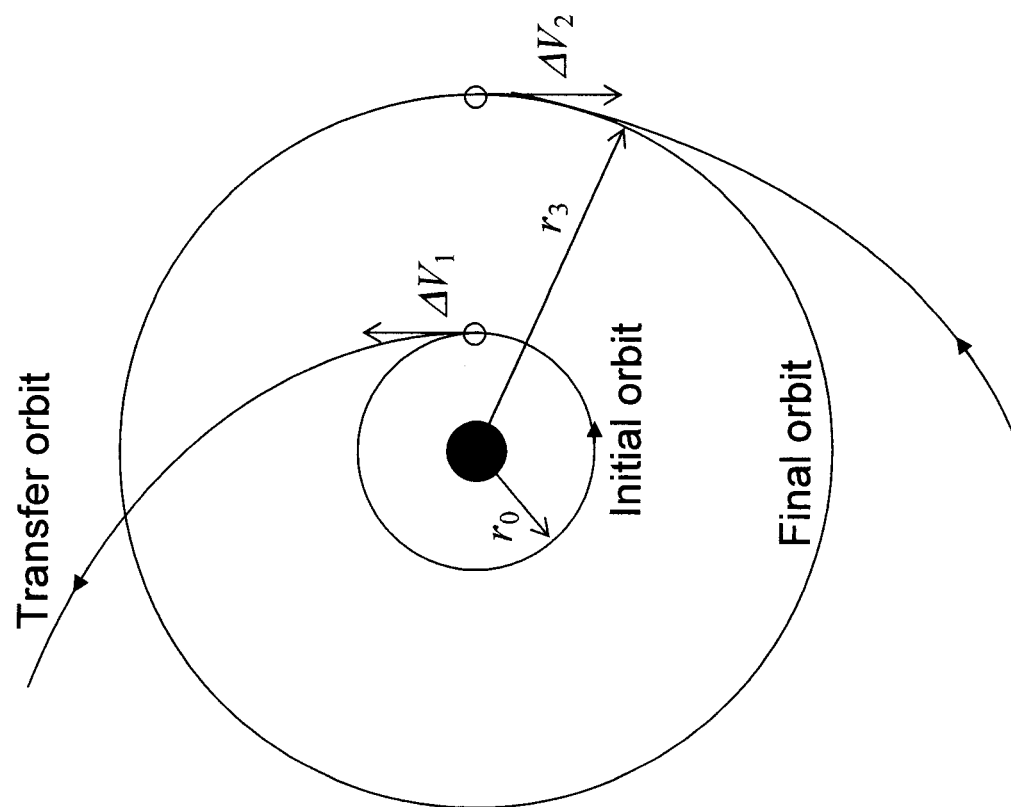


Fig. 6. Biparabolic transfer: Ascending case.

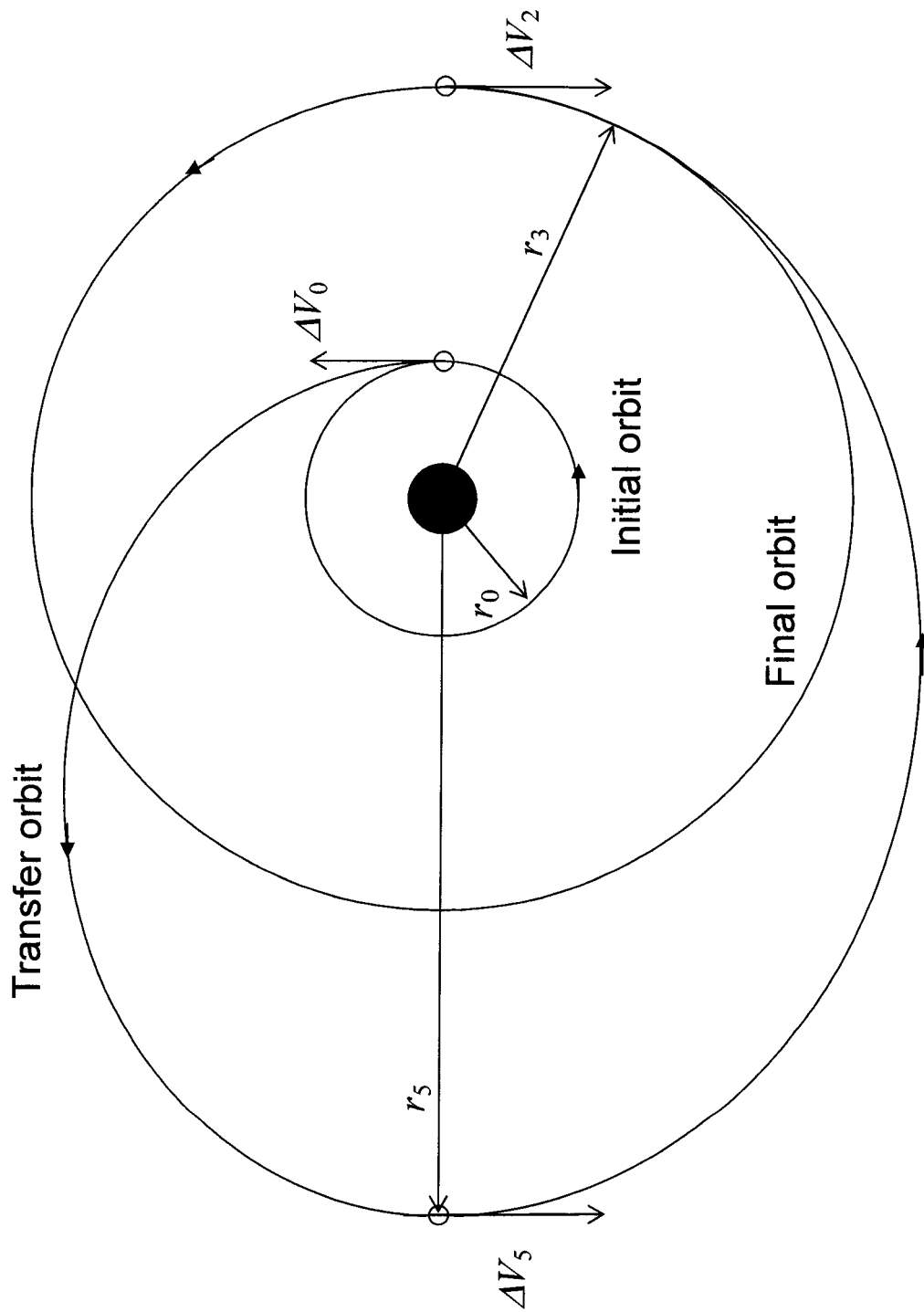


Fig. 7. Bielliptic transfer: Ascending case.